LA-UR -85-3525

CONF-850277--5

LA-UR--85-3525

DE86 002386

NOV 08 1985

Los Alamos National Laboratory is operated by the University of California for the United States Department of Energy under contract W-7405-ENG-36

TITLE SOLAR WIND - MAGNETOSPHERE COUPLING AND THE DISTANT MAGNETOTAIL: ISEE-3 OBSERVATIONS

AUTHOR(S) J.A. Slavin, E.J. Smith, D.G. Sibeck, D.N. Baker
R.D. Zwickl, S.I. Akasofu, and R.P. Lepping



SUBMITTED TO Solar Wind-Magnetosphere Coupling
Pasadena, CA, February 2-15, 1985.



Los Alamos Los Alamos National Laboratory
Los Alamos, New Mexico 87545

FORM NO. 836 R4
ST. NO. 2629 5/81

# SOLAR WIND - MAGNETOSPHERE COUPLING AND THE DISTANT MAGNETOTAIL: ISEE-3 OBSERVATIONS

J.A. Slavin and E.J. Smith

Jet Propulsion Laboratory
California Institute of Technology
Pasadena, California 91109

D.G. Sibeck

Department of Atmospheric Sciences
University of California
Los Angeles, California 90024

D.N. Baker and R.D. Zwickl

Los Alamos National Laboratory
University of California
Los Alamos, New Mexico

S.I. Akasofu
University of Alaska
Fairbanks, Alaska

R.P. Lepping
NASA Goddard Space Flight Center
Greenbelt, Maryland

Submitted to SOLAR WIND-MAGNETOSPHERE COUPLING

May, 1985

Revised September, 1985

## Abstract

ISEE-3 Geotail observations are used to investigate the relationship between the interplanetary magnetic field, substorm activity, and the distant magnetotail. Magnetic field and plasma observations are used to present evidence for the existence of a quasi-permanent, curved reconnection neutral line in the distant tail. The distance to the neutral line varies from $|X|=120-140\ R_e$ near the center of the tail to beyond $|X|=200\ R_e$ at the flanks. Downstream of the neutral line the plasma sheet magnetic field is shown to be negative and directly proportional to negative $B_z$ in the solar wind as observed by IMP-8. $V_x$ in the distant plasma sheet is also found to be proportional to IMF $B_z$ with southward IMF producing the highest anti-solar flow velocities. A global dayside reconnection efficiency of $20 \pm 5$ % is derived from the ISEE-3/IMP-8 magnetic field comparisons. Substorm activity, as measured by the AL index, produces enhanced negative $B_z$ and tailward $V_x$ in the distant plasma sheet in agreement with the basic predictions of the reconnection-based models of substorms. The rate of magnetic flux transfer out of the tail as a function of AL is found to be consistent with previous near-earth studies. Similarly, the mass and energy fluxes carried by plasma sheet flow down the tail are consistent with theoretical mass and energy budgets for an open magnetosphere. In summary, the ISEE-3 Geotail observations appear to provide good support for reconnection models of solar wind - magnetosphere coupling and substorm energy rates.

## Introduction

Most theories of solar wind - magnetosphere coupling are based upon the early works of Dungey (1961) and Axford and Hines (1961). In both cases the solar wind exerts normal and tangential stresses on the geomagnetic field which compress most of the field lines to form the dayside magnetosphere, but with some fraction being pulled downstream to produce the magnetotail. However, while Axford and Hines suggested that the tangential stress is due to quasi-viscous forces operating at the magnetopause, Dungey proposed that plasma processes exist which allow interplanetary and geomagnetic field lines to "merge" at the dayside magnetopause. Merging produces "open" field lines which have one foot rooted in the planet and the other in the solar wind. The existence of open field lines enables the solar wind to exert a drag on the magnetosphere via simple JxB forces. The open field lines are then pulled back into the tail where they eventually "reconnect" to produce closed geomagnetic field lines which convect back toward the dayside magnetosphere and interplanetary field lines which move tailward to rejoin the solar wind.

Two decades of magnetospheric research have produced considerable evidence that both the reconnection and viscous interaction processes are important for solar wind - magnetosphere coupling. However, it appears that reconnection plays the dominant role, particularly during storms and substorms (Cowley, 1982). Given this picture of the interaction, it has been possible to conduct quantitative studies of the global magnetospheric energy budget (Stern, 1984). While knowledge of how magnetospheric energy is dissipated in the upper atmosphere/ionosphere has

reached a fairly mature state (Perreault and Akasofu, 1978), comparativeley little is known about the downstream boundary condition on this system, the distant magnetotail. In this study observations from the recent ISEE-3 Geotail Mission are analyzed for the purposes of (1) testing the predictions of the reconnection models of solar wind - magnetosphere coupling, and (2) investigating the rates of mass and energy loss down the distant plasma sheet as a function of substorm activty. Overall, the results are generally consistent with the reconnection-based models of the magnetosphere and they indicate a close coupling between the solar wind, the near-earth magnetosphere, and the distant magnetotail.

## Quasi-permanent Distant Neutral Line

After four years at the forward sun-earth Lagrange point, ISEE-3 was moved into the magnetotail where it spent part of 1982 and most of 1983 (Bame et al., 1983; Slavin et al., 1983; Scholer et al., 1983). Although the analysis of observations from this mission is still at an early stage, many studies of distant magnetotail properties and phenomena have already been published (e.g. Cowley et al., 1984; Hones et al., 1984; Scholer et al., 1984; Baker et al., 1984; Slavin et al., 1984; Tsurutani et al., 1984; Sibeck et al, 1984; Feldman et al., 1984; Smith et al., 1984; Daly et al., 1984). Briefly stated, ISEE-3 made two deep tail orbits with apogees in the 220-240 $R_e$ range and a number of lower apogee orbits. For the purpose of this study, the 25 December 1982 - 20 April 1983 interval covering approximately the first half of the mission will be used. Detailed studies of the evolution of plasma and magnetic field parameters within the various regions of the tail have already been conducted (Zwickl et al., 1984; Slavin et al., 1985) and should be referred to for more detailed information on the instruments, trajectory, and general properties of the tail.

The top panel of Figure 1 displays a schematic view of the classical open magnetosphere. The two principal regions of the tail are the lobes and the plasma sheet. Magnetic merging at the dayside magnetopause creates open field lines which are pulled back to form the lobes. The low beta ($\beta=nk(T_e+T_i)/(B^2/8\pi)$) lobes are separated by a high beta region termed the plasma sheet. The particles in the plasma sheet are of solar wind and ionospheric origin with ExB drift toward the X-Y plane concentrating them in the plasma sheet (Hill, 1974; Pilipp and Morfill, 1978). The addition of particles to the plasma sheet is balanced in two ways: 1) particles entering the plasma sheet earthward of the neutral line are eventually convected back to the forward magnetosphere where they are lost to precipitation or pass into the magnetosheath, and 2) particles entering the plasma sheet tailward of the neutral line are convected down the tail to rejoin the solar wind.

Similarly, the transport of magnetic field lines into the tail is, on averge, balanced by reconnection at a neutral line in the nightside magnetosphere. Two lobe field lines reconnect to produce a closed field line which moves back toward the Earth and an interplanetary field line which returns to the solar wind. During substorms additional neutral lines are thought to form in the near-earth magnetotail (Russell and

McPherron, 1973), but there is disagreement concerning site and dynamics of the merging process (e.g. Frank et al., 1976; Hones et al., 1977).

The ISEE-3 Geotail observations have provided the first opportunity to confirm and quantify the nightside half of the open magnetosphere hypothesis with in situ measurements. For the purpose of identifying the average location of the distant neutral line all of the plasma sheet intervals in the ISEE-3 data set were identified as in Slavin et al. (1985). Two parameters, $B_z$ in GSM coordinates and flow speed normalized to the local Alfven speed, i.e. $M_A$, have been averaged into ten earth radii bins and plotted against the X coordinate of spacecraft postion. The magnetic field observations were made by the JPL VHM magnetometer and the bulk flow parameters were derived from the LANL electron plasma measurements as described by Zwickl et al. (1984). Bame et al. (1984), Cowley et al. (1984), Scholer et al. (1984), Daly et al. (1984), and Zwickl et al. (1984) have already established that plasma sheet bulk flow velocity becomes largely tailward in direction beyond $|X|=100\ R_e$. In the bottom panels of Figure 1 it is further shown that the flow also becomes super-Alfvenic near that distance and $B_z$ ceases to be strongly northward. These results are all consistent with lack of closed field lines tailward of approximately $|X|=100\ R_e$ (Cowley et al., 1984; Zwickl et al., 1984; Slavin et al., 1985) and the reported observation of reconnection slow mode shocks (Feldman et al., 1984; Smith et al., 1984).

However, the failure of $B_z$ to become negative at the point where the flow becomes super-Alfvenic and tailward does represent a difficulty for the existence of a quasi-permanent neutral line across the full width of the tail at $|X|=100\ R_e$. The behavior of the magnetic field is further investigated in Figure 2 where $B_z$ is plotted against the Y coordinate of spacecraft position for three ranges in $|X|$. The results indicate that $B_z$ did indeed turn negative beyond $|X|=100\ R_e$, but only near the east - west center of the plasma sheet. Furthermore, the width of the region of negative $B_z$ appears to increase with growing distance from the Earth. The top panel shows the corresponding reconnection neutral line shape in the X - Y plane (Slavin et al., 1985) where a parabola has been fit to the two observations of neutral line width. The curved nature of the resulting neutral line tends to focus the anti-solar flow tailward of the neutral line to produce the easily observable high speed flow away from the Earth. The flow direction is observed to be tailward across the entire width of the plasma sheet (Slavin et al., 1985), and hence, we do not expect that the neutral line stretches across the the entire width of the tail. Rather, the closed field lines being pulled downstream at the flanks of the tail must eventually break-off due to reconnection closer to the earth and probably near the central portion of the tail. The existence of a curved neutral line has been suggested previously on the basis of energetic particle observations (Russell, 1977) and is generally attributed to the warping effect of closed field lines dragged down the flanks of the tail by the viscous component of the solar wind interaction with the magnetosphere. Finally, the bottom panel of Figure 2 displays cuts through the tail parallel to the Y-Z plane at three downstream distances. The plasma sheet starts out on closed field lines, but is gradually consumed by a growing region of interplanetary field lines as the length of the neutral line in the Y direction increases. Eventually, the width of the region of reconnected field lines

spreads across more than half of the tail and causes the averages as a function of X in Figure 1 to go negative at $|X|>200\ R_e$. In this model the entire region separating the two lobes is composed of interplanetary field lines and magnetospheric debris, such as plasmoids, by $|X|=300\text{-}400\ R_e$. This flow of plasma and magnetic field out the back of the magnetosphere represents mass and energy derived from the solar wind that did not reach the Earth and must be taken into account in the magnetospheric energy budget.

## Distant Tail Response to IMF $B_z$

Southward IMF upstream of the Earth results in dayside reconnection which transfers magnetic field lines to the tail as already discussed. Studies of the dayside magnetopause and the near tail have measured the rates at which magnetic flux is transfered to the tail and returned to the forward magnetosphere (Fairfield and Ness, 1970; Caan et al., 1973; Holzer and Slavin, 1978; Slavin and Holzer, 1979). In this study we investigate, for the first time, the final portion of the magnetic flux transfer cycle; the rate of magnetic flux return to the solar wind via the flow of reconnected flux tubes out the rear of the tail. Three plasma sheet parameters are plotted against upstream $B_z$ in Figure 3. The IMF observations were provided by the GSFC fluxgate magnetometer on IMP-8. The ISEE-3 plasma sheet observations are limited to the $|X|>100\ R_e$ and $30>Y>0\ R_e$ region. Based upon the results shown in the previous two figures this data selection criteria should result in the analysis being limited mostly to the region tailward of the distant neutral line. Using hourly averaged IMP-8 measurements with a time delay of 1 hour, these procedures yielded 392 ISEE-3 5 minute averaged values with which to conduct the analysis. The plasma sheet parameters considered were $B_z$, $V_x$, and the magnetic flux transfer rate, $\Phi_T(\mathrm{Mx/s}) = B_z(\mathrm{nT})\ V_x(\mathrm{km/s})\ 30(R_e)\ 6380\times10^5(\mathrm{cm}/R_e)$. Hence, a net transport of southward magnetic flux ($B_z<0$) out of the tail ($V_x<0$) corresponds to a positive flux transfer rate, $\Phi_T$.

As shown in Figure 3, all three plasma sheet quantities, $B_z$, $V_x$, and $\Phi_T$, are correlated with solar wind $B_z$. The linear least square regressions in each case are:

$$B_z(\text{ISEE-3; nT}) = 0.17(\pm.02)\ B_z(\text{IMP-8; nT}) - 0.05(\pm.06)\ (\text{nT})$$

$$V_x(\text{ISEE-3; km/s}) = 36(\pm4.8)\ B_z(\text{IMP-8; nT}) - 411(\pm13)\ (\text{km/s}) \qquad (1)$$

$$\Phi_T(\text{ISEE-3;Mx/s}) = -0.20(\pm.03)\times10^{13}B_z(\text{IMP-8;nT}) + 0.24(\pm.07)\times10^{13}(\text{Mx/s})$$

The correlation coefficients are 0.4 in each of the three cases. Although there is considerable unexplained variance, these correlations are significant at the >99% confidence level (Bevington, 1969). Accordingly, it appears that conditions in the distant plasma sheet exhibit the same strong dependence upon upstream $B_z$ as has been observed elsewhere in the magnetosphere. In particular, if it is assumed that plasma sheet flow speed and solar wind flow were comparable, then an average dayside reconnection efficiency of 17 ± 2% is implied by the regression of ISEE-3 $B_z$ on IMP-8 $B_z$. However, if instead an average solar wind

speed of 430 km/s is assumed, then the bottom panel of Figure 3 indicates that the overall efficiency of the dayside merging process is 24 $\pm$ 4%. Combining these results to get an average efficiency of 20 $\pm$ 5% yields excellent agreement with previous estimates based upon studies of dayside cusp motion (Burch, 1973), magnetopause erosion (Holzer and Slavin, 1978), and magnetospheric dawn-dusk electric field (Lei et al., 1981) and demonstrates strong observational internal consistency for the open model of the magnetosphere.

## Distant Tail Response to Substorm Activity

Whether the energy is stored (Caan et al., 1973) or directly supplied (Akasofu, 1983), overall magnetospheric power dissipation increases dramatically during substorms. The reconnection-based models of the substorm process require additional neutral lines to form in the near tail giving rise to magnetic islands termed plasmoids which then move rapidly away from the Earth and down the tail (e.g. Birn and Hones, 1981). Under these circumstances the occurrence of substorm activity is expected to produce rapid plasma flow away from the Earth and southward magnetic fields in the distant tail. Studies of the cis-lunar plasma sheet following substorm onset have resulted in mixed results (e.g. Nishida and Nagayama, 1973; Caan et al., 1979; Lui et al., 1977). However, the ISEE-3 measurements at $|X|>100\ R_e$ offer an advantage for this type of study in that the spacecraft is generally tailward of the region(s) where reconnection is taking place as discussed earlier. Under these circumstances motion of the neutral line back and forth over the spacecraft will not interfere with the correlative studies.

For the purpose of monitoring substorm occurrence and intensity, a nine station AE index was constructed at the University of Alaska. The interval considered was days 1-55, 1983 which corresponded approximately to the period when ISEE-3 was at $|X|>200\ R_e$ during its first deep tail orbit. The stations used were Narssarssuaq, Abisko, Dixon Island, Tixie Bay, College, Yellowknife, Fort Churchill, Great Whale River, and Leirvogur. Overall, the coverage provided by these nine stations is quite good and they provide a reasonable proxy for the standard 12 station AE which is not yet available for 1983. Based upon previous ISEE-3 studies (Baker et al., 1984; Slavin et al., 1985), a 30 minute lag was assumed for the propagation of substorm effects to $|X|=200\ R_e$ (i.e. an average speed of 700 km/s; see the plasma sheet flow speeds for $B_z<0$ in Figure 3). In Figure 4 plasma sheet $B_z$, $V_x$, and $\Phi_T$ measured at ISEE-3 are displayed as a function of the |AL| index. The AL index, a measure of westward electrojet intensity, was chosen because of its simpler interpretation relative to AE and past successes in relating this index to magnetospheric processes (e.g. Slavin and Holzer, 1979). As with the IMP8 /ISEE-3 correlations in the previous figure, there is considerable scatter present in all three panels. However, clear dependences on AL are present with linear regression analyses yielding:

$$\begin{aligned} B_z(\text{ISEE-3; nT}) &= -0.12(\pm.03)\times10^{-2}\ |AL|(\text{nT}) - 0.04(\pm.08)\ (\text{nT}) \\ V_x(\text{ISEE-3; km/s}) &= -0.63(\pm.05)\ |AL|\ (\text{nT}) - 326(\pm16)\ (\text{km/s}) \\ \Phi_T(\text{ISEE-3; Mx/s}) &= 0.13(\pm.03)\times10^{11}\ |AL|\ (\text{nT}) + 0.22(\pm.09)\times10^{13}\ (\text{Mx/s}) \end{aligned} \qquad (2)$$

with fair to poor correlation coefficients of 0.2, 0.5, and 0.2, respectively. In each case, increased substorm activity was followed by enhanced anti-sunward flows and negative $B_z$ in the distant tail as predicted by the reconnection models. Furthermore, there is excellent agreement with previous near-earth studies as to the rate of magnetic flux transport into and out of the magnetotail as a function of AL (Slavin and Holzer, 1979).

Mass and Energy Loss Down the Tail

It has long been recognized that not all of the mass and energy transfered from the solar wind to the magnetotail is eventually deposited in the ionosphere and upper atmosphere (Siscoe and Cummings, 1969). In addition to earthward flow, nightside reconnection also generates the tailward flow considered in detail by this study. Energy budget calculations for the magnetosphere typically assume that the Poynting flux across the magnetopause earthward of the neutral line eventually reaches the Earth while energy entering downstream of the neutral line simply returns to interplanetary space. If this hypothesis is correct, and the distance to the neutral line in the central regions of the tail is 120-140 $R_e$ as shown in Figures 1 and 2, then by $|X|=200$ $R_e$ the flux of energy returning to the solar wind may approach equality with the sunward flux earthward of the neutral line which is ultimately dissipated in the ionosphere and upper atmosphere (i.e., both are fed by the Poynting flux through an approximately 100 $R_e$ segment of magnetotail). Similar arguments apply to the entry of solar wind plasma into the magnetosphere (Pilipp and Morfill, 1978) as discussed earlier.

For the purpose of investigating magnetospheric losses due to plasma sheet flow away from the Earth, two additional plasma sheet parameters have been examined as a function of substorm activity. The first is simply the mass flux, $nV_x$. The second is the net energy flux down the tail, $U_T = V_x(nm_pV^2 + B^2/8\pi + nkT_e)$. The thermal energy of the ions has been neglected because it is not measured by ISEE-3. As before, five minute averages of the ISEE-3 magnetic field and plasma measurements were used and the analyis was limited to the central portion (i.e. $30>Y>0$ $R_e$) of the distant (i.e. $|X|>200$ $R_e$) plasma sheet. In this case, however, AE was used as the substorm index due to its being preferred by many studies considering total energy dissipation rates (Perreault and Akasofu, 1978; Wei et al., 1985).

The results in Figure 5 show no dependence of mass flux on AE. At these distances the flux of particles away from the Earth is relatively constant near $10^7/cm^2$-s. Assuming a width of 30 $R_e$ for the region of tailward flow and a plasma sheet thickness of 2 $R_e$, or slightly less than the 3 $R_e$ observed at $|X|=60$ $R_e$ by Rich et al. (1973), the total plasma sheet loss rate is $2.4 \times 10^{26}$ particles/s. This number is roughly similar to that believed to be lost out of the plasma sheet earthward of the neutral line (Hill, 1974). Hence, the plasma sheet mass flux observations at $|X|=200$ $R_e$ support the models where a neutral line with an average position of 120-140 $R_e$ partitions the magnetosphere with respect to the mass budget.

The correlation between plasma sheet energy flux, $U_T$, and AE is somewhat better:

$$U_T(\text{ISEE-3;ergs/cm}^2\text{-s}) = 0.25(\pm.08)\times10^{-4}\text{AE(nT)} + 0.24(\pm.02)\times10^{-1}(\text{ergs/cm}^2\text{-s}) \quad (3)$$

but with a correlation coefficient of only 0.2. Making the same assumptions as before regarding the cross section of the flow region, the total energy loss to plasma sheet flow away from the Earth is $6\text{-}12\times10^{17}$ ergs/s or $6\text{-}12\times10^{10}$ Watts. This rate of energy loss to the solar wind is very similar to the ionospheric joule heating which takes place during AE levels of 200-1000 nT (i.e. $4\text{-}20\times10^{10}$ W; Wei et al., 1985) and, therefore the Poynting flux entering the magnetotail earthward of the distant neutral line. As with the mass flux case, the distant plasma sheet energy fluxes appear to be consistent with previous magnetospheric energy budget calculations (Siscoe and Cummings, 1969; Stern, 1984). In addition, Feldman et al. (1984) have inferred dissipation rates of $10^{17}$-$10^{18}$ erg/s based on the observation of slow mode shocks in the the ISEE-3 distant tail measurements.

## Summary

ISEE-3 magnetic field and plasma observations in the distant plasma sheet have been used to test some of the predictions of the reconnection models of solar wind - magnetosphere coupling and the substorm process. In particular, we have investigated the position and shape of the distant neutral line and the dependence of conditions in the distant plama sheet upon IMF $B_z$ and the AE/AL index. The results have supported the existence of a curved distant neutral line whose distance to the Earth varies from 120-140 $R_e$ near the center of the tail to more than 200 $R_e$ at the flanks (Figures 1-2). At $|X|>100$ $R_e$ both $B_z$ and $V_x$ are directly proportional to IMF $B_z$ measured at IMP-8 (Figure 3). Similarly, $B_z$ and $V_x$ in the distant plasma sheet are also proportional to the level of substorm activity as measured by the AL index (Figure 4). Finally, the rates at which magnetic flux, mass, and energy are being returned to the solar wind via flow away from the Earth in the distant plasma sheet are all found to be in good agreement with expectation based upon the open model of the magnetosphere (Figure 5). Hence, the results of this study provide good support for the reconnection-based models of solar wind - magnetosphere coupling and the substorm process.

Acknowledgements. The research described in this report was carried out at the Jet Propulsion Laboratory of the California Institute of Technology under contract to the National Aeronautics and Space Administration. The work at Los Alamos National Laboratory was performed under the auspices of the U.S. Department of Energy with support from NASA.

## References

Akasofu, S.-I., Solar wind disturbances and the solar wind-magnetosphere energy coupling function, Space Sci. Rev., 34, 173, 1983.

Axford, W.I., and C.O. Hines, A unifying theory of high latitude geophysical phenomena and geomagnetic storms, Can. J. Phys., 3, 1433, 1961.

Baker, D.N., S.J. Bame, R.D. Belian, W.C. Feldman, J.T. Gosling, P.R. Higbie, E.W. Hones, Jr., D.J. McComas, and R.D. Zwickl, Correlated dynamical changes in the near Earth and distant magnetotail regions: ISEE-3, J. Geophys. Res., 89, 3855, 1984.

Bame, S.J., R.C. Anderson, J.R. Asbridge, D.N. Baker, W.C. Feldman, J.T. Gosling, E.W. Hones, Jr., D.J. McComas, and R.D. Zwickl, Plasma regimes in the deep geomagnetic tail: ISEE-3, Geophys Rev. Lett., 10, 912, 1983.

Birn, J., and E.W. Hones, Jr., Three dimensional computer modeling of dynamic reconnection in the geomagnetic tail, J. Geophys. Res., 86, 6802, 1981.

Burch, J.L., The rate of erosion of dayside magnetic flux based upon a quantitative study of the dependence of polar cusp latitude on the IMF, Radio Sci., 8, 955, 1973.

Caan, M.N., R.L. McPherron, and C.T. Russell, Solar wind and substorm related changes in the lobes of the geomagnetic tail, J. Geophys. Res., 78, 8087, 1973.

Caan, M.N., D.H. Fairfield, and E.W. Hones, Jr., Magnetic fields in flowing magnetotail plasmas and their significance for magnetic reconnection, J. Geophys. Res., 84, 1971, 1979.

Cowley, S.W.H., The causes of convection in the Earth's magnetosphere: A review of recent developments during the IMS, Rev. Geophys. Space Phys., 20, 531, 1982.

Cowley, S.W.H., R.J. Hynds, I.G. Richardson, P.W. Daly, T.R. Sanderson, K.-P. Wenzel, J.A. Slavin, and B.T. Tsurutani, Energetic ion regimes in the deep geomagnetic tail: ISEE-3, Geophys. Res. Lett., 11, 275, 1984.

Daly, P.W., T.R. Sanderson, and K.-P. Wenzel, Survey of energetic (E>35 keV) ion anisotropies in the deep geomagnetic tail, J. Geophys. Res., 89, 19733, 1974.

Dungey, J.W., Interplanetary magnetic field and the auroral zones, Phys. Rev. Lett., 6, 3913, 1965.

Fairfield, D.H., and N.F. Ness, Configuration of the geomagnetic tail during substorms, J. Geophys. Res., 75, 7032, 1970.

Feldman, W.C., D.N. Baker, S.J. Bame, J. Birn, E.W. Hones, Jr., S.J. Schwartz, and R.L. Tokar, Power dissipation at slow mode shocks in the distant geomagnetic tail, Geophys. Res. Lett., 11, 1058, 1984.

Frank, L.A., K.L. Ackerson, and R.P. Lepping, On hot tenuous plasmas, fireballs, and boundary layers in the Earth's magnetotail, J. Geophys. Res., 81, 5859, 1976.

Hill, T.W., Origin of the plasma sheet, Rev. Geophys. Space Phys., 12, 379, 1974.

Holzer, R.E., and J.A. Slavin, Magnetic flux transfer associated with expansions and contractions of the dayside magnetosphere, J. Geophys. Res., 83, 3831, 1978.

Hones, E.W., Jr., Substorm processes in the magnetotail: Comments on 'On hot tenuous plasmas fireballs, and boundary layers in the Earth's magnetotail' by L.A. Frank, K.L. Ackerson, and R.P. Lepping, J. Geophys. Res., 82, 5633, 1977.

Hones, E.W., Jr., D.N. Baker, S.J. Bame, W.C. Feldman, J.T. Gosling, D.J. McComas, R.D. Zwickl, J.A. Slavin, E.J. Smith, and B.T. Tsurutani, Structure of the magnetotail at 220 $R_e$ and its response to geomagnetic activity, J. Geophys. Res., 11, 5, 1984.

Lei, W.R. Gendrin, B. Higel, and J. Berchem, Relationships between the solar wind electric field and the magnetospheric convection electric field, Geophys. Res. Lett., 8, 1099, 1981.

Lui, A.T.Y., C.-I. Meng, and S.-I. Akasofu, Search for the magnetic neutral line in the near Earth plasma sheet, 3. An extensive study of magnetic field observations at lunar distances, J. Geophys. Res., 82, 3603, 1977.

Nishida, A., and N. Nagayama, Synoptic survey of the neutral line in the magnetotail during substorm expansion phase, J. Geophys. Res., 78, 3782, 1973.

Perreault, P., and S.-I. Akasofu, A study of geomagnetic storms, Geophys. J. R. Astron. Soc., 54, 547, 1978.

Pilipp, W.G., and G. Morfill, The formation of the plasma sheet resulting from plasma mantle dynamics, J. Geophys. Res., 83, 5671, 1978.

Rich, F.J., D.L. Reasoner, and W.J. Burke, Plasma sheet at lunar distance: Characteristics and interactions with lunar surface, J. Geophys. Res., 78, 8097, 1973.

Russell, C.T., and R.L. McPherron, The magnetotail and substorms, Space Sci. Rev., 15, 205, 1973.

Russell, C.T., Some comments on the topology of the geomagnetic tail, J. Geophys. Res., 82, 1625, 1977.

Scholer, M., G. Gloeckler, D. Hovestadt, F.M. Ipavich, B. Klecker, and C.Y. Fan, Anisotropies and flows of suprathermal particles in the distant magnetotail: ISEE-3 observations, Geophys. Res. Lett., 10, 1203, 1983.

Scholer, M., G. Gloeckler, D. Hovestadt, B. Klecker, and F.M. Ipavich, Characteristics of plasmoid-like structures in the distant magnetotail, J. Geophys. Res., 89, 8872, 1984.

Sibeck, D.G., G.L. Siscoe, J.A. Slavin, E.J. Smith, S.J. Bame, and F.L. Scarf, Magnetotail flux ropes, Geophys. Res. Lett., 11, 1090, 1984.

Siscoe, G.L., and W.D. Cummings, On the cause of geomagnetic bays, Planet. Space Sci., 17, 1795, 1969.

Slavin, J.A., and R.E. Holzer, Empirical relationships between interplanetary conditions, magnetospheric flux transfer, and the AL index, Quantitative Modeling of Magnetospheric Processes, ed. W.P. Olson, pp. 423-436, AGU, Washington, D.C., 1979.

Slavin, J.A., B.T. Tsurutani, E.J. Smith, D.E. Jones, and D.G. Sibeck, Average configuration of the distant ($<220$ $R_e$) magnetotail: Initial ISEE-3 magnetic field results, Geophys. Res. Lett., 10, 973, 1983.

Slavin, J.A., E.J. Smith, B.T. Tsurutani, D.G. Sibeck, H.G. Singer, D.N. Baker, J.T. Gosling, E.W. Hones, Jr., and F.L. Scarf, Substorm associated traveling compression regions in the distant tail: ISEE-3 Geotail observations, Geophys. Res. Lett., 11, 657, 1984.

Slavin, J.A., E.J. Smith, D.G. Sibeck, D.N. Baker, R.D. Zwickl, and S.-I. Akasofu, An ISEE-3 study of average and substorm conditions in the distant magnetotail, J. Geophys. Res., in press, 1985.

Smith, E.J., J.A. Slavin, B.T. Tsurutani, W.C. Feldman, and S.J. Bame, Slow mode shocks in the Earth's magnetotail: ISEE-3, Geophys. Res. Lett., 11, 1054, 1984.

Stern, D.P., Energetics of the magnetosphere, NASA Tech. Memorandum 86067, 1984.

Tsurutani, B.T., D.E. Jones, and D.G. Sibeck, The two lobed structure of the distant ($X>200$ $R_e$) magnetotail, Geophys. Res. Lett., 11, 1066, 1984.

Wei, S., B.-H. Ahn, and S.-I. Akasofu, The global joule heat production rate and the AE index, Planet. Space Sci., 33, 279, 1985.

Zwickl, R.D., D.N. Baker, S.J. Bame, W.C. Feldman, J.T. Gosling, E.W. Hones, Jr., D.J. McComas, B.T. Tsurutani, and J.A. Slavin, Evolution of the Earth's distant magnetotail:ISEE-3 electron plasma results, J. Geophys. Res., 1984.

Figure Captions

Figure 1. The top panel displays a cut through the center of the magnetosphere parallel to the GSM X-Z plane. The plasma sheet has been shaded and flow directions are indicated by arrows on either side of the distant neutral line. The bottom panels plot mean $B_z$ and Alfvenic Mach number observed by ISEE-3 in the plasma sheet as a function of X. The close correspondence between where the flow speed becomes super-Alfvenic and $B_z$ ceases to be strongly northward mark the average location of the distant neutral line, $|X|=100\text{-}140\ R_e$.

Figure 2. The top panel displays a cut through the center of the magnetosphere parallel to the GSM X-Y plane. A dashed line indicates the shape of the distant neutral line suggested by the ISEE-3 magnetotail observations with arrows indicating flow direction. In the middle panel mean plasma sheet $B_z$ is plotted as a function of GSM Y for three different ranges in X. Earthward of $|X|=100\ R_e$ the magnetic field is northward everywhere. However, at greater distances $B_z$ becomes negative in a region near the center of the tail that grows in Y as |X| increases. Finally, the bottom panel displays cuts through the magnetotail parallel to the Y-Z at several downstream distances. The magnetic field topology implied by the curved neutral line model is indicated by stiple for closed field (i.e. plasma sheet) regions, NL(SL) for north (south) lobe open field lines, and I for interplanetary (i.e. disconnected) field lines moving to rejoin the solar wind.

Figure 3. Five minuted averaged $B_z$, $V_x$, and flux transfer rate, $\Phi_T$, observed by ISEE-3 in the plasma sheet at $|X|>100\ R_e$ and $30\geq Y\geq 0\ R_e$ are plotted against 1 hour averaged IMP-8 GSM $B_z$ with a time lag of 1 hour. The linear fits to the data are described in the text.

Figure 4. Five minute averaged $B_z$, $V_x$, and flux transfer rate, $\Phi_T$, observed by ISEE-3 in the plasma sheet at $|X|\geq 200\ R_e$ and $30\geq Y\geq 0\ R_e$ are plotted against five minute averaged |AL| with a time lag of 30 minutes. The linear fits to the data are described in the text.

Figure 5. Five minute averaged anti-solar mass and energy flux observed by ISEE-3 in the plasma sheet at $|X|\geq 200\ R_e$ and $30\geq Y\geq 0\ R_e$ are plotted against five minute averaged AE with a 30 minute time lag. The linear fits to the data are desribed in the text.

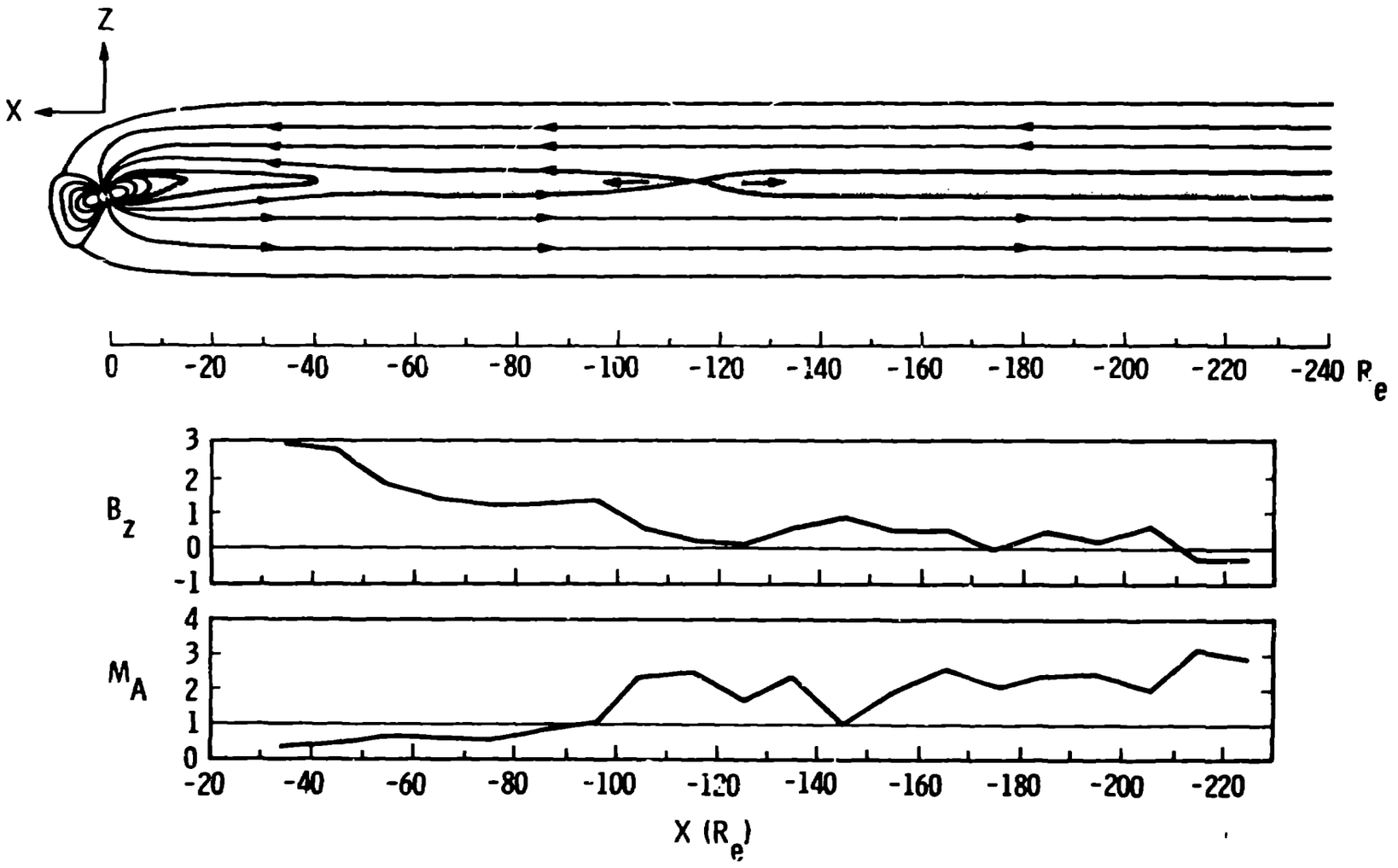
Z
X
0 -20 -40 -60 -80 -100 -120 -140 -160 -180 -200 -220 -240 $R_e$
$B_z$
3 2 1 0 -1
$M_A$
4 3 2 1 0
-20 -40 -60 -80 -100 -120 -140 -160 -180 -200 -220
X ($R_e$)

Figure 1.

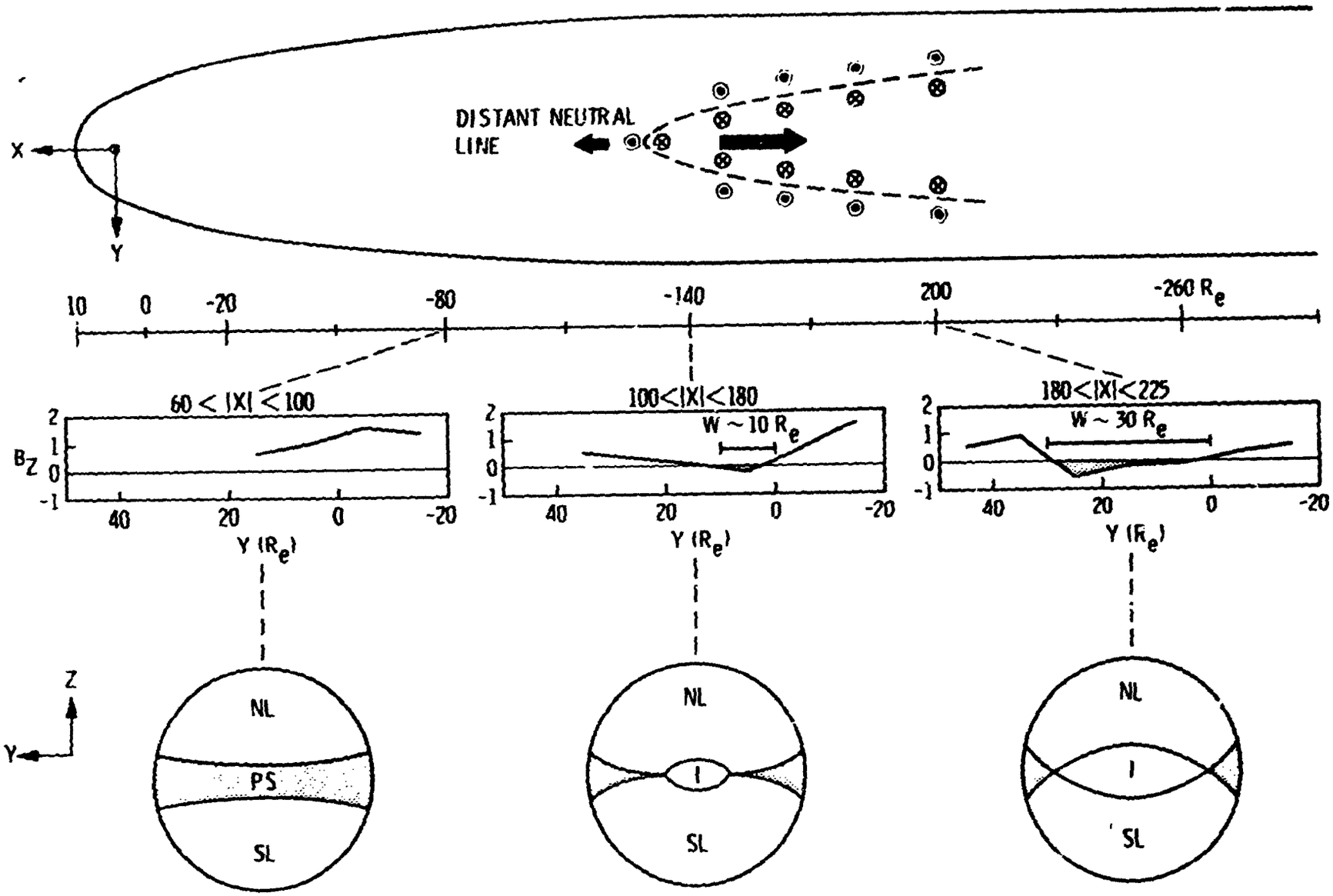
DISTANT NEUTRAL LINE
X
Y
10
0
-20
-80
-140
200
-260 $R_e$
60 < |X| < 100
100<|X|<180
180<|X|<225
W ~ 10 $R_e$
W ~ 30 $R_e$
$B_Z$
Y ($R_e$)
Z
Y
NL
PS
SL
I

Figure 2.

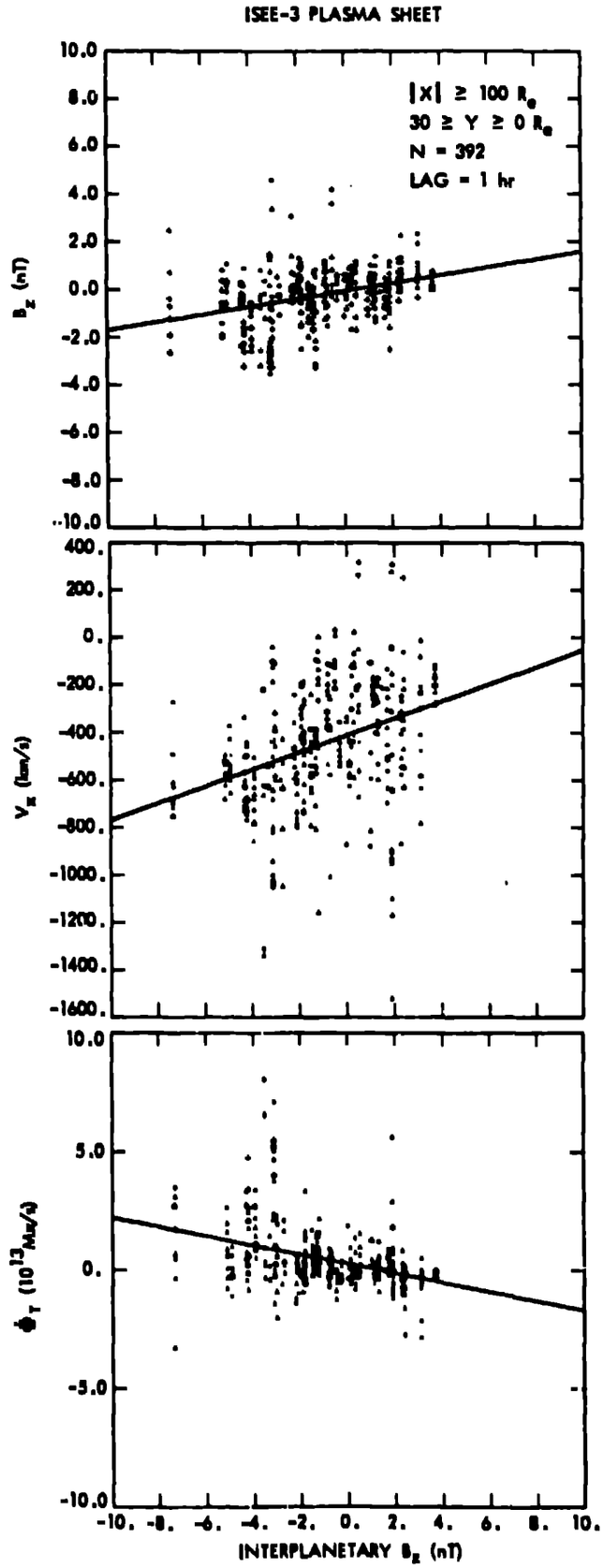
ISEE-3 PLASMA SHEET
|X| ≥ 100 R_e
30 ≥ Y ≥ 0 R_e
N = 392
LAG = 1 hr
B_z (nT)
V_x (km/s)
Φ_T (10^13 Mx/s)
INTERPLANETARY B_z (nT)

Figure 3.

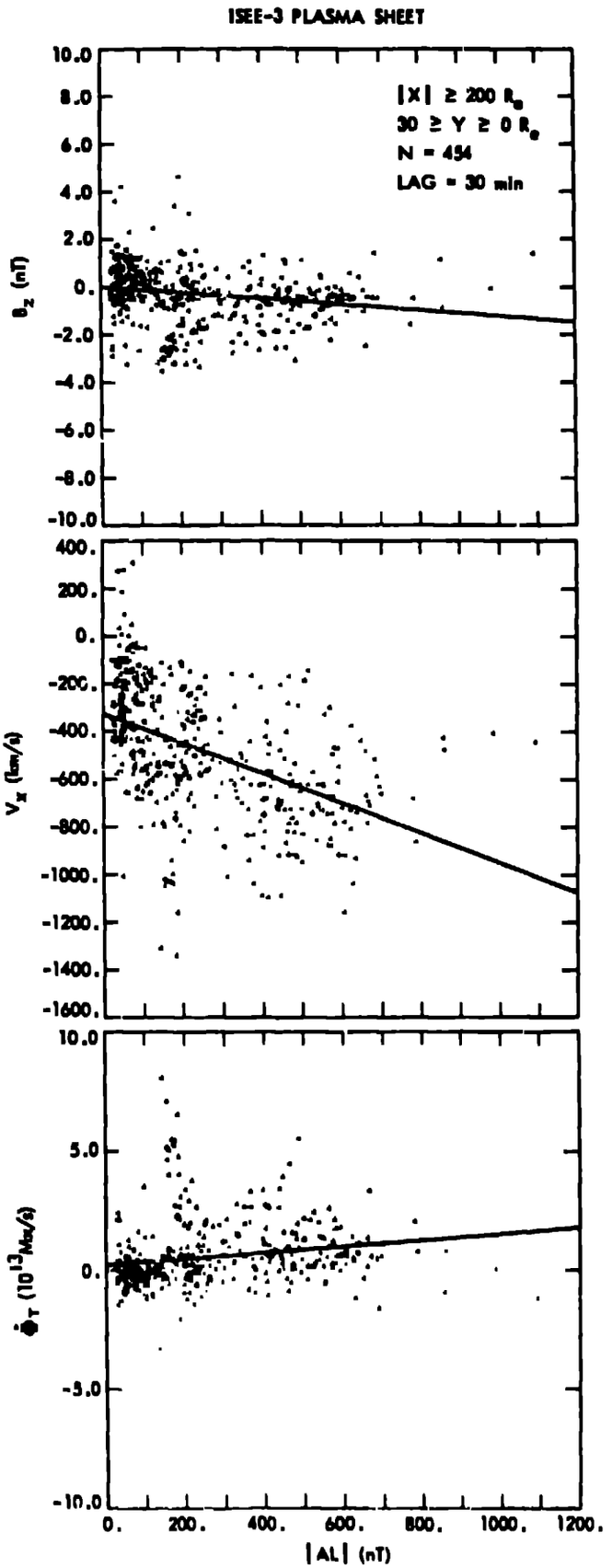
ISEE-3 PLASMA SHEET
|X| ≥ 200 R_E
30 ≥ Y ≥ 0 R_E
N = 454
LAG = 30 min
B_Z (nT)
V_X (km/s)
Φ_T (10^13 Mx/s)
|AL| (nT)

Figure 4.

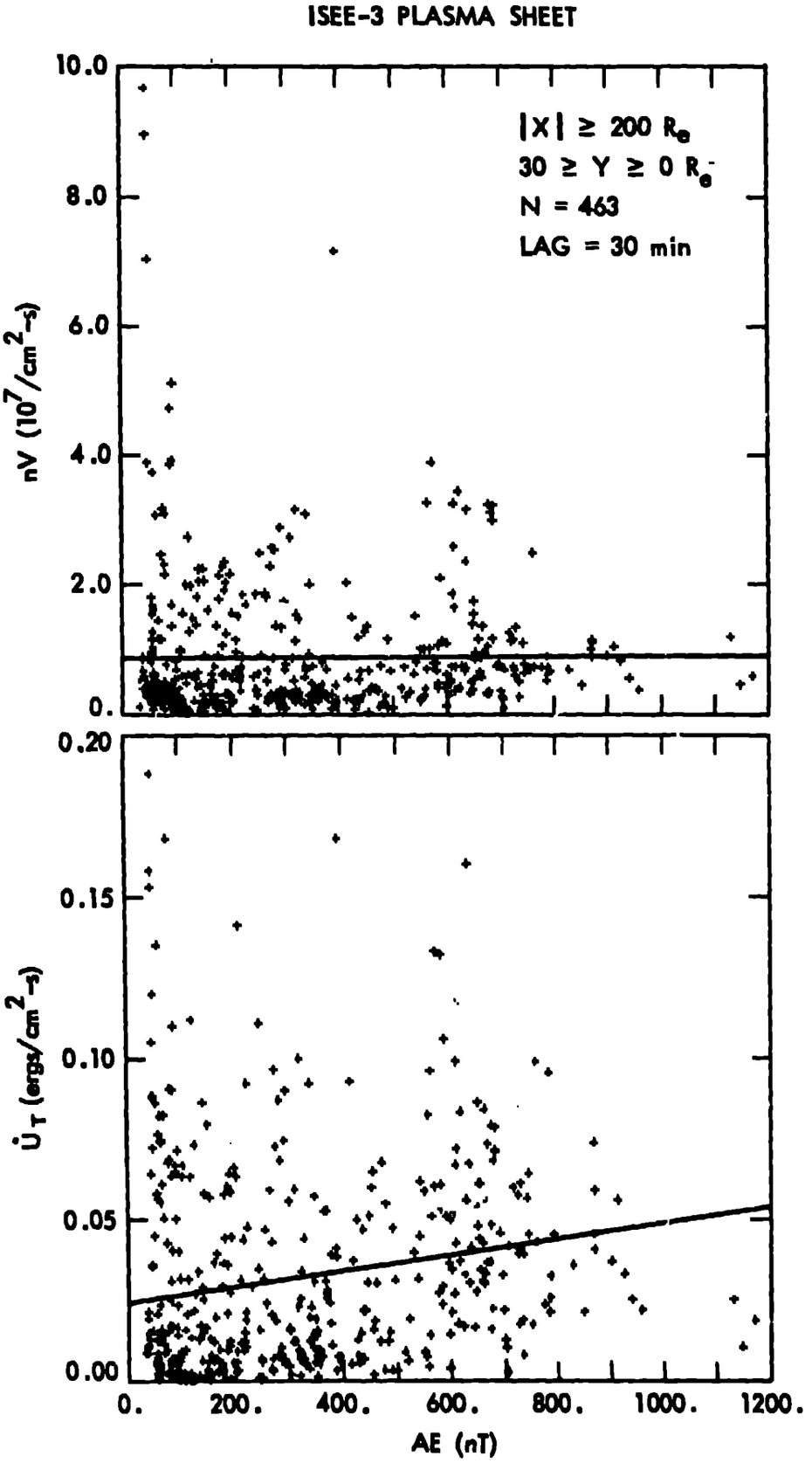
ISEE-3 PLASMA SHEET
|X| ≥ 200 Re
30 ≥ Y ≥ 0 Re
N = 463
LAG = 30 min
nV (10^7/cm^2-s)
10.0
8.0
6.0
4.0
2.0
0.
0.20
0.15
0.10
0.05
0.00
U̇T (ergs/cm^2-s)
0.
200.
400.
600.
800.
1000.
1200.
AE (nT)

Figure 5.